

Upgradation of bauxite by molecular hydrogen and hydrogen plasma

B.R. Parhi¹, S.K. Sahoo¹, S.C. Mishra¹, B. Bhoi², R.K. Paramguru³, and B.K. Satapathy⁴

1) Department of Metallurgical and Materials Engineering, National Institute of Technology, Rourkela 769008, Odisha, India

2) Institute of Minerals and Materials Technology, Bhubaneswar 751013, Odisha, India

3) Kalinga Institute of Industrial Technology, Bhubaneswar 751024, Odisha, India

4) National Aluminium Company Ltd., Bhubaneswar 751013, Odisha, India

(Received: 7 January 2016; revised: 9 April 2016; accepted: 22 May 2016)

Abstract: An approach was developed to upgrade the bauxite ore by molecular hydrogen and hydrogen plasma. A gibbsite-type bauxite sample was obtained from National Aluminium Company (NALCO), Odisha, India. The obtained sample was crushed and sieved (to 100 μm) prior to the chemical analysis and grain-size distribution study. The bauxite sample was calcined in the temperature range from 500 to 700°C for different time intervals to optimize the conditions for maximum moisture removal. This process was followed by the reduction of the calcined ore by molecular hydrogen and hydrogen plasma. Extraction of alumina from the reduced ore was carried out via acid leaching in chloride media for 2 h at 60°C. X-ray diffraction, scanning electron microscopy, thermogravimetry in conjunction with differential scanning calorimetry, and Fourier transform infrared spectroscopy were used to determine the physicochemical characteristics of the material before and after extraction. Alumina extracted from the reduced ore at the optimum calcination temperature of 700°C and the optimum calcination time of 4 h is found to be 90% pure.

Keywords: upgrading; bauxite; calcination; leaching; alumina; extraction

1. Introduction

Bauxite is a rich source of alumina for producing aluminum. Because it is a naturally occurring mineral, it contains numerous impurities such as silica, iron, titania, phosphorous, calcium, sulfur, magnesium, and various carbonate and silicate minerals. These impurities in the bauxite not only create the quality problems but also cause the environmental pollution and increase the production costs. Hence, the removal of these impurities from bauxite is necessary during the beneficiation process [1].

The extraction of alumina from bauxite is basically an upgradation process that involves the separation of alumina from the undesirable bauxite constituents such as the oxides of iron, titanium, silicon, calcium, vanadium, and manganese. [2]. Bayer's process is the major industrial technique used to refine bauxite to produce alumina. In this process, bauxite ore is digested in a solution of sodium hydroxide (NaOH). During caustic digestion, the amphoteric aluminum oxide passes into the solution as soluble sodium alu-

minate [3]. The alkaline solution is subsequently treated with carbon dioxide to precipitate aluminum hydroxide. Aluminum hydroxide decomposes into aluminum oxide when heated to 980°C, giving off water vapor in the process. However, the production of alumina from bauxite ores via this process consumes a large amount of caustic soda and generates a huge amount of slurry waste called red mud. Red mud discharged by the alumina industry poses the environmental and ecological threats [4–8] because of its high alkalinity ($10 \leq \text{pH} \leq 12.5$). Hence, the proper utilization and value-added metal recovery from red mud have become objectives of several researchers [9–19]. The production of aluminum involves the commercial technology of bauxite purification to produce alumina by removing unwanted impurities followed by the smelting of alumina to produce aluminum. These technologies involve various disadvantages, including high energy consumption, emissions of large amounts of greenhouse gases, emissions of harmful fluorides, and the generation of a huge amount of slurry waste [20–22].

Corresponding author: B.R. Parhi E-mail: basudevpubikash@gmail.com

© University of Science and Technology Beijing and Springer-Verlag Berlin Heidelberg 2016

Hence, an appropriate bauxite beneficiation process wherein the impurities such as oxides of iron, silicon, and titanium can be transformed into suitable value-added products is needed. Some researchers have recently attempted to develop the alternative methods for bauxite reduction. Among the developed methods, natural gas and plasma technologies have been adopted for the reduction of metal oxides [23]. The thermal plasma method has been in extensive industrial-scale applications because of its unique features, including the high temperatures, the generation of excited and ionized atoms, the steep temperature gradient, and the generation of high-thermal-conductivity plasma; this method opens a favorable pathway for metallurgical reactions, especially the reduction of metal oxides [23]. However, very limited work has been reported on the reduction of metal oxides by plasma technology using hydrogen as a reducing agent.

Bhoi *et al.* [24] have investigated the direct reduction of iron through hydrogen plasma treatment. They developed a green process for the preparation of direct-reduced iron (DRI) by reducing iron ore using microwave-assisted low-temperature hydrogen plasma. Lyubochko *et al.* [25] proposed a method for reducing aluminum oxide in non-equilibrium hydrogen plasma in a combined glow discharge (CGD) at a pressure ranging from 1315.8 to 13158 Pa at a discharge current ranging from 5×10^{-2} to 3 A and a hydrogen flow rate ranging from 10^{-6} to 10^{-4} nm³/s. A high conversion degree of aluminum oxide to aluminum was achieved (60%), with an energy consumption of 20 kWh/kg of Al₂O₃. Gold *et al.* [26] studied the reduction of iron oxide powders to molten iron by hydrogen and natural gas. Sabat *et al.* [27] reported the reduction of cobalt oxide (Co₃O₄) to cobalt metal via low-temperature hydrogen plasma. Nakamura *et al.* [28] carried out smelting reduction of iron ore using Ar-H₂ plasma and concluded that the utilization efficiency of hydrogen was higher than the value estimated by thermodynamic equilibrium for H₂-H₂O-Fe-Fe_xO by the effect of atomic hydrogen on the reduction. Huczko *et al.* [29] investigated the processing of silica in radio-frequency (rf) plasma using a new experimental system in which the process was carried out entirely in the vapor phase. They obtained SiO or Si by either thermal decomposition of SiO₂ or reduction by H₂.

Apart from the aforementioned studies, hydrogen as a reducing agent has several potential advantages [30–31]. First, the reaction of metal oxides with hydrogen is far more environmentally friendly than reduction with carbon-containing compounds, because the byproduct is water rather than carbon dioxide. Hydrogen in the form of plasma

(consisting of H₂, H, and H⁺) is a very powerful reductant that can reduce most metal oxides at temperatures below the melting points of metals. Because the hydrogen in atomic and ionic form lies lower than the positions of most other atoms and ions in the Ellingham diagram, it can reduce most metal oxides. Hence, we have attempted to reduce bauxite ore with molecular hydrogen and hydrogen plasma.

In the present study, the bauxite was upgraded by extracting alumina from the reduced bauxite followed by leaching with 3 mol/L HCl. Bauxite was reduced with molecular hydrogen followed by hydrogen plasma.

2. Materials and methods

2.1. Materials

Mineral samples obtained from National Aluminium Company (NALCO), Odisha, India were crushed and powdered using a planetary ball mill. Milling was carried out for 2 h. The powdered bauxite was then completely dried at 150°C and sieved using different sieves to determine the grain size distribution.

2.2. Chemical analysis

Common analytical methods were employed for the chemical analysis of the bauxite sample. For chemical analysis, 2 g bauxite sample was mixed with fusion mixture (1:1 Na₂CO₃ and K₂CO₃ by mass) by heating at 1000°C in a platinum crucible. The mixture was subsequently dissolved in hydrochloric acid solution for quantitative determination of the bauxite sample's components. In addition, a small amount of bauxite sample was heated in a platinum crucible to 700°C for 1 h. During this process, the total heat loss due to dehydration or decomposition was determined.

2.3. Calcination studies

The powdered samples and the pellets were subsequently calcined at 700°C for 4 h to remove the moisture and volatile matter present in the samples. Pellets were prepared from the bauxite powder by using uniaxial cold compaction with a load of 6.5 t. Notably, a series of calcination experiments were conducted at different temperatures and for different time periods to remove all of the moisture and volatile matter present in the samples. It was observed that calcination at 700°C for 4 h was sufficient to remove almost all of the moisture and volatile matter present in a given sample.

2.4. Reduction studies

The bauxite samples were subjected to ball milling in a planetary ball mill for 2 h to obtain bauxite powder for the

treatment with molecular hydrogen. The bauxite sample was heated in a muffle furnace at 650°C for 2 h under the hydrogen gas flowing at 2 m³/h, as shown in Fig. 1. Pellets with a diameter and thickness of 20 mm and 4 mm, respectively, were prepared from the bauxite powders by uniaxial cold compaction for hydrogen plasma processing.



Fig. 1. Muffle furnace for molecular hydrogen processing of bauxite samples.

The bauxite pellets were reduced with hydrogen plasma in a microwave hydrogen plasma reactor. The reactor included two parts: the reactor chamber, where the plasma was formed and the reduction occurred, and the operation rack, which regulated the working parameters of the experiment. A quartz ring surrounding the copper plate aided in focusing the plasma on the sample. In all experiments, the sample was placed on a molybdenum sample holder positioned within the plasma region and the chamber was closed after the sample was placed on the holder. The chamber was then evacuated, and a base pressure of 0.1 Pa was maintained inside the chamber by a rotary pump. The operation rack incorporated a microwave generator with a 6000 W power supply. A magnetron was used to generate microwaves of standard frequency of $2.54 \times 10^9 \text{ s}^{-1}$; the microwaves were guided by a waveguide to the sample chamber. In the chamber, the high-frequency microwaves were interacted with the incoming hydrogen gas (99.999% pure) supplied to the reactor to produce the hydrogen plasma. The plasma plume covered the total surface of pellet, where the reduction occurred.

2.5. Alumina extraction studies

Calcined bauxite powder was reduced with molecular hydrogen and hydrogen plasma. The reduced bauxite powder was treated at 60°C with 3 mol/L hydrochloric acid for 2 h under magnetic stirring. Solid–liquid separation was then

carried out to separate the mixture via filtration. Alumina, along with silica, was separated as residue, leaving behind iron and titanium in the filtrate as their chlorides.

2.6. Physicochemical characterization

Particle size analysis of the residue sample was performed on a Netzsch Nano-zetasizer. X-ray diffraction (XRD) patterns of the bauxite samples before and after reduction were recorded using a Panalytical X'pert PW 3040/00 system equipped with a Cu K_α radiation source. The scans were recorded in the 2θ range from 10° to 100°. The surface morphology of the bauxite samples was determined by scanning electron microscopy (SEM, JEOL JSM-6480 LV). Differential scanning calorimetry (DSC) and thermogravimetry (TG) (Perkin Elmer Diamond) analyses were carried out under the inert atmosphere over the temperature range from 30 to 1450°C at a heating rate of 10°C·min⁻¹. Fourier transform infrared (FTIR) spectra of the alumina samples were collected using a Thermo Fisher Nicolet IS 10 spectrophotometer.

3. Results and discussion

3.1. Physicochemical analysis of bauxite sample

Fig. 2 shows the XRD pattern and SEM image, respectively, of the raw bauxite sample. The XRD data in Fig. 2(a) show that the material is predominantly composed of gibbsite (Al(OH)₃) along with iron in the form of hematite (Fe₂O₃). Peaks attributable to TiO₂ and SiO₂ are not detected by XRD because of their low mass fractions, as shown in Table 1. However, the mass fractions of TiO₂ and SiO₂ were confirmed from the wet chemical analysis of the bauxite sample; the analysis results are presented in Table 1. The surface morphology of sample was analyzed by SEM. As observed in Fig. 2(b), the particles exhibit the irregular shapes with different sizes. After grinding the sample to smaller than 100 μm, the grain size distribution of sample was determined by sieving it via sieves of different sizes.

3.2. Calcination studies

Bauxite samples with different particle sizes were calcined at 500, 600, and 700°C; in each case, the samples were analyzed at different time intervals of 2, 3, and 4 h to determine the optimal calcination conditions. The results, which are shown in Fig. 3, reveal that the samples sieved to less than 100 μm easily lost water because of their smaller particle sizes. Nonetheless, the water removal continues to 700°C. Hence, the optimum calcination conditions were chosen as 700°C and 4 h.

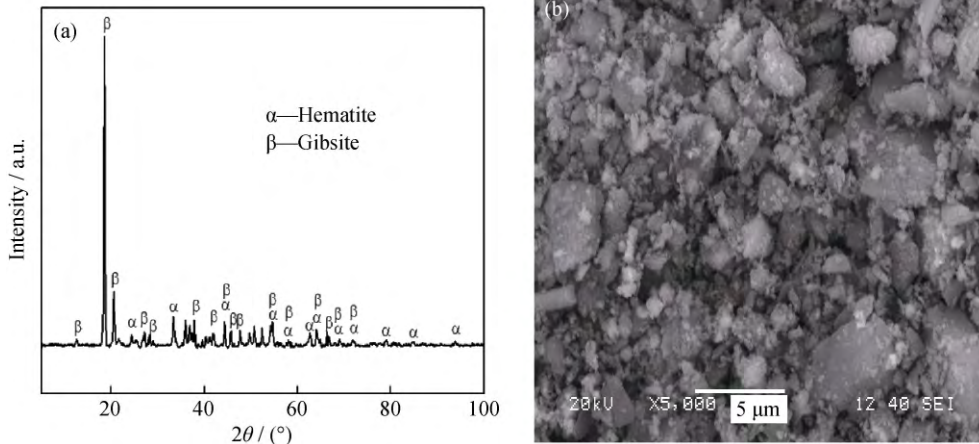


Fig. 2. (a) XRD pattern and (b) SEM micrograph of the bauxite sample.

Table 1. Chemical composition of bauxite used in the present study

	wt%				
	Al ₂ O ₃	Fe ₂ O ₃	TiO ₂	SiO ₂	LOI
	43	23	3	4	22.5

Note: LOI is loss on ignition.

The XRD pattern in Fig. 4 shows that the calcined material is predominantly comprised of aluminum and iron in their oxide forms. As shown the TG–DSC results in Figs.

5(a) and (b), two phase changes associated with the mass loss/decomposition of the samples are observed in the temperature ranges from 300 to 400°C and from 500 to 600°C, respectively. These phase changes are clearly confirmed by the appearance of an endothermic peak at 380°C (DSC) associated with the dissociation or decomposition of gibbsite, whose dissociation temperature is very similar to that of goethite, followed by another endothermic peak at 580°C due to the dissociation of boehmite. The DTG curve of

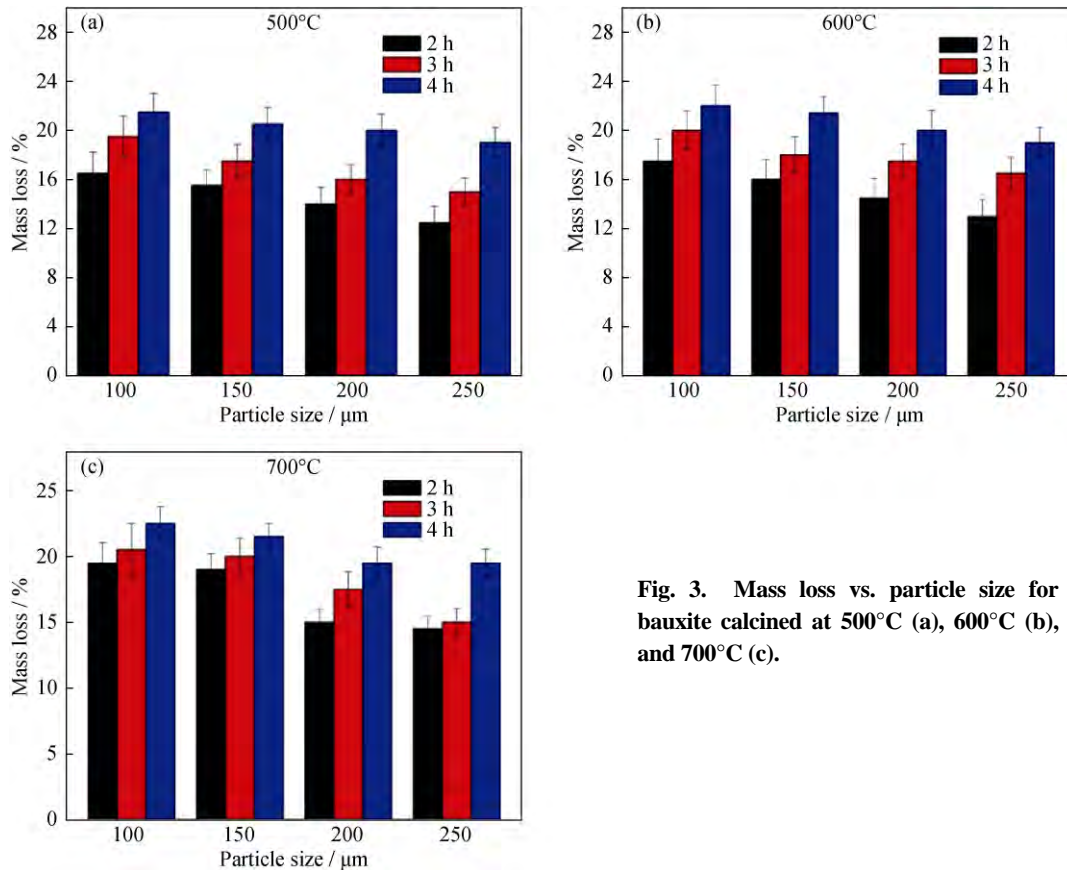


Fig. 3. Mass loss vs. particle size for bauxite calcined at 500°C (a), 600°C (b), and 700°C (c).

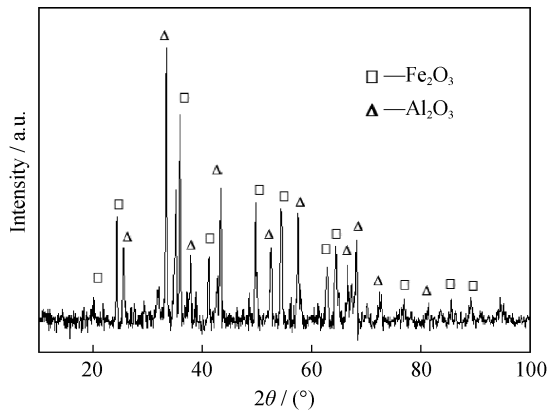


Fig. 4. XRD pattern of a bauxite sample calcined at 700°C.

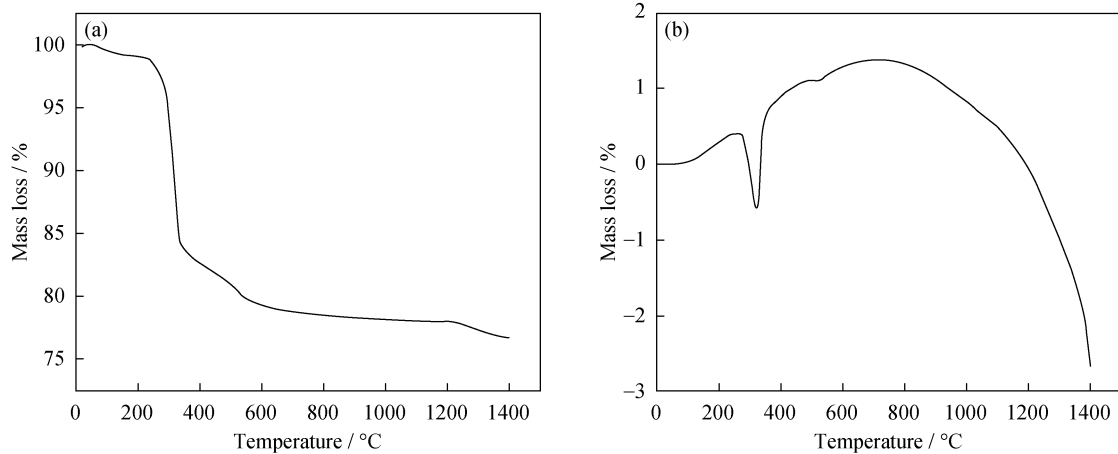


Fig. 5. TG (a) and DSC (b) curves of bauxite calcined at 700°C.

3.3. Reduction of bauxite using molecular hydrogen and hydrogen plasma

Fig. 6 shows the XRD pattern of reduced bauxite after reduction processing by molecular hydrogen. The XRD patterns of samples after reduction processing are dominated by iron (Fe) and Al_2O_3 peaks. XRD patterns of reduced bauxite pellets at the different temperatures are presented in Fig. 7, non-reduction of Al_2O_3 is present in the bauxite sample. Both Fe and Al_2O_3 peaks are observed in the XRD patterns of samples. The ability of Fe_2O_3 to be reduced can be explained by the consideration of Ellingham diagram, which shows that the standard free energy change (ΔG^\ominus) for the formation of Fe_2O_3 is -397.48 kJ/mol; this value is substantially less negative than those of other oxides presence in bauxite, which are -849.35 kJ/mol for SiO_2 and -1054.37 kJ/mol for Al_2O_3 , respectively. Hence, the reducibility of Fe_2O_3 through hydrogen plasma is greater than the reducibilities of SiO_2 , TiO_2 , and Al_2O_3 .

3.4. Alumina extraction studies

Alumina was extracted from the reduced bauxite through

bauxite in Fig. 5(b) exhibits a sharp endothermic peak at 380°C due to the dehydration of hydrated alumina, followed by a small endotherm at 520°C due to the dehydroxylation of boehmite phase. The corresponding differential thermal analysis (DTA) trace exhibits two sharp endothermic peaks that characterize the thermal nature of the bauxite sample. Dehydration in this case involves the loss of actually adsorbed as well as the interlayer water and the removal of hydroxyl water. The first endothermic peak at 380°C is due to the discharge of adsorbed water molecules. The second endothermic peak at 520°C is related to the removal of hydroxyl groups.

acid leaching with 3 mol/L HCl at 60°C for 2 h. After the acid leaching of reduced bauxite, the filtrate contained chlorides of iron; Al_2O_3 was present in the residue, along with other minor oxides. The filtrate was subsequently treated with NaOH to precipitate iron hydroxide ($\text{Fe}(\text{OH})_3$), which was subsequently converted into Fe_2O_3 upon further heating. The particle size of the residue calcined at 900°C was

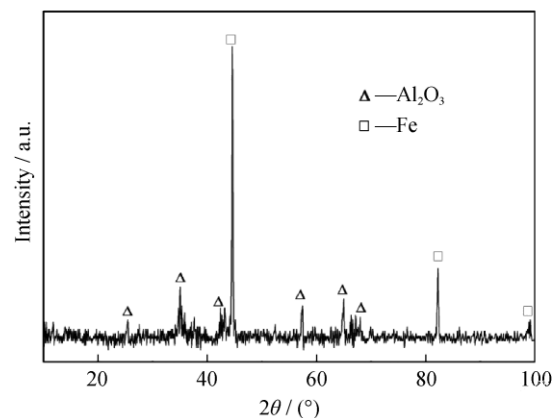


Fig. 6. XRD pattern of the reduced bauxite after reduction processing at 650°C for 2 h under the hydrogen flowing at 2 m^3/h .

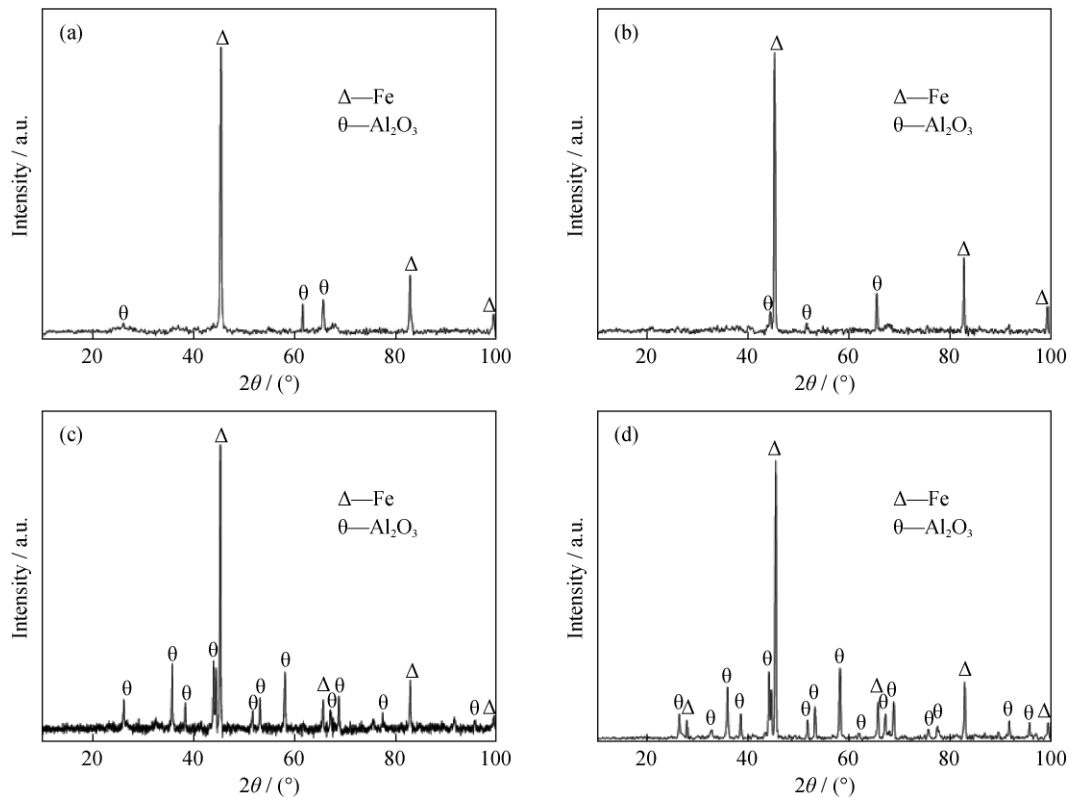


Fig. 7. XRD patterns of the reduced bauxite pellets after reduction processing by hydrogen plasma at a pressure of 5332.88 Pa with a hydrogen flow rate of 250 cm³/min for 1 h at the temperatures of 700°C (a), 900°C (b), 1000°C (c), and 1200°C (d).

measured using a zeta-sizer; the results are shown in Fig. 8. As evident in the figure, a small peak is observed at approximately 100–800 nm and a large peak is observed at approximately 3000–7000 nm. The average particle size of the alumina extracted from the reduced bauxite was measured as 5.3 μm.

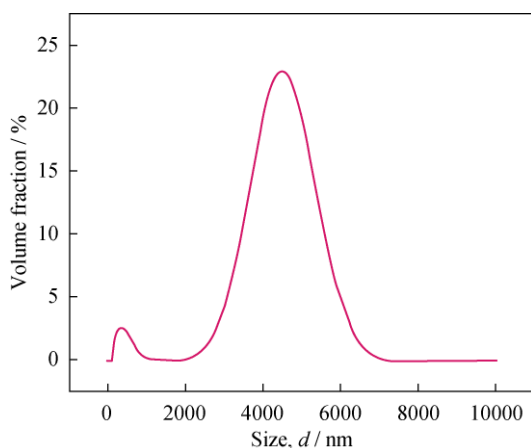


Fig. 8. Particle size measurement of alumina generated by leaching of reduced bauxite.

The residue after acid leaching was analyzed by XRD; the results are shown in Fig. 9. Al₂O₃ peaks dominate the

pattern. TiO₂ and SiO₂ peaks are not observed in the XRD pattern because of their low mass fractions, which are below the detection limit of the diffractometer. Wet chemical analysis of the residue in Table 2 confirms the presence of TiO₂ (2wt%) and SiO₂ (3.59wt%) in lower mass fractions, and the purity of alumina is determined to be 90%.

Fig. 10 shows the thermal analysis (TG and DSC) results for the alumina sample. All alumina phases are involved in

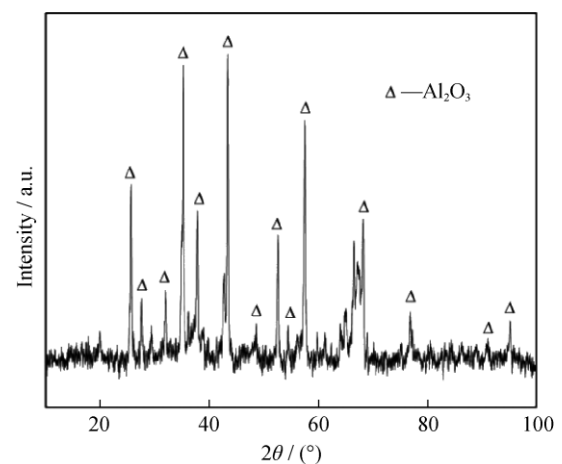


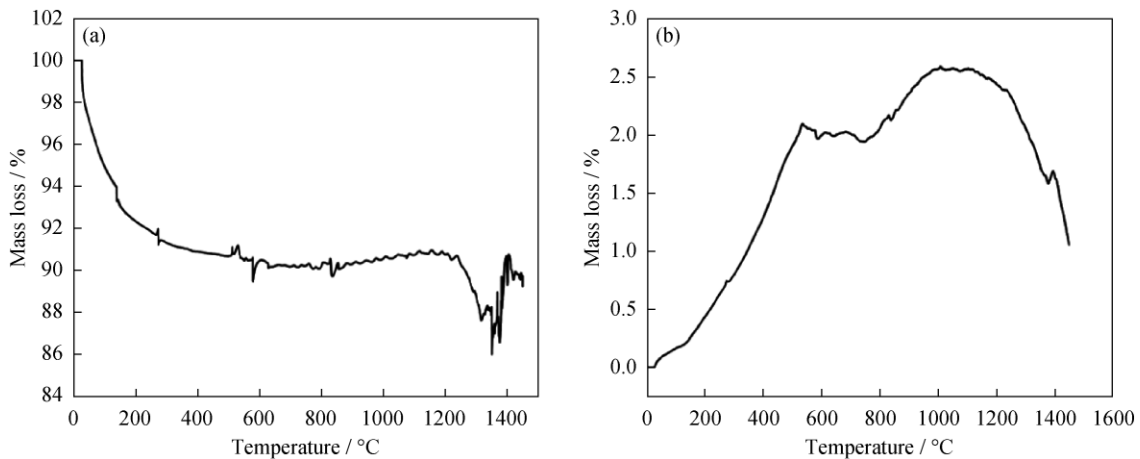
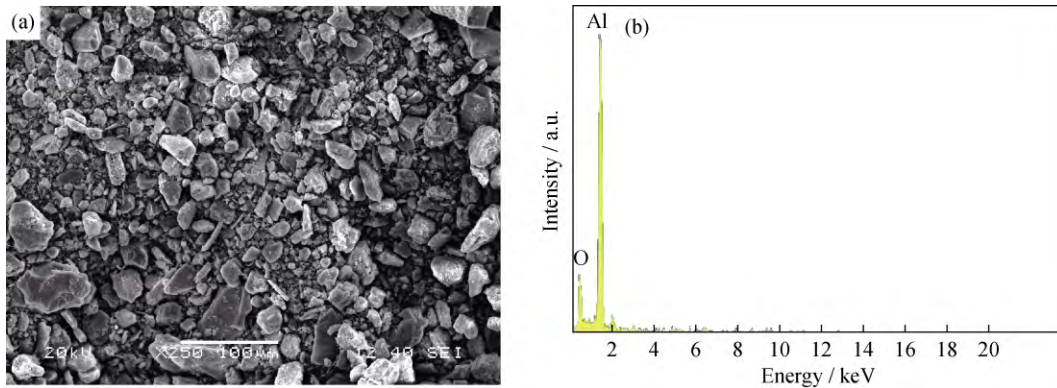
Fig. 9. XRD pattern of alumina generated by leaching of reduced bauxite.

Table 2. Chemical composition of alumina obtained after leaching

wt%				
Al ₂ O ₃	Fe ₂ O ₃	TiO ₂	SiO ₂	LOI
89.88	1.5	2	3.59	2.26

the transformation sequences, which are ended in α -phase alumina at high temperatures [32]. An exothermic peak is observed at 380°C, which indicates the amorphous nature of alumina. Again, the exothermic and endothermic peaks are

observed at 510°C and 590°C, which indicates the conversion of alumina to γ -alumina. The endothermic peak at 840°C indicates the conversion of alumina to both δ - and θ -alumina, and another endothermic peak at 1330°C indicates the existence of α -alumina, as shown in Figs. 10(a) and (b). Fig. 11 shows an SEM micrograph and the EDX spectrum of the extracted alumina, respectively. The SEM image shows a granular-type structure of the alumina, and the EDS spectrum confirms this result.

**Fig. 10. TG (a) and DSC (b) curves of alumina generated by leaching of reduced bauxite.****Fig. 11. SEM micrograph (a) and EDX spectrum (b) of alumina generated by leaching of reduced bauxite.**

3.5. FTIR study of extracted alumina

Fig. 12 shows the Fourier transform infrared spectrum (FTIR) of alumina produced by leaching of reduced bauxite. The Al₂O₃ spectrum shows a broad band in the range from 533.17 to 806.44 cm⁻¹, which confirms the existence of an amorphous structure or disordered defects. The FTIR peaks at 533.17, 560.62, 576.18, and 598.84 cm⁻¹ are assigned to the stretching mode of Al–O in an octahedral arrangement, and the bands at approximately 806.44 and 1081.25 cm⁻¹ are related to Al–O stretching modes of tetrahedra. The previously reported range for stretching modes associated with

Al–O–Al linkages is 633.68 to 864.44 cm⁻¹ [33]. The peak at 560.62 cm⁻¹ observed in this work is attributed to Al–O stretching. The peaks at 1637.52 and 3407.64 cm⁻¹ are attributed to the impurities. These FTIR results confirm the presence of alumina in the specimen.

4. Conclusions

The particle size of the bauxite sample used in this study is 100 μ m, which is smaller than that of the bauxite sample used in Bayer's process (149 μ m). The alumina content of the mineral is found to be 43wt% by chemical analysis;

however, after the leaching process of the same sample, the extracted alumina is found to be 89.88wt% pure. XRD studies reveal that this alumina is associated with gibbsite. Similarly, it is found that the bauxite specimen contains 23wt% hematite (Fe_2O_3), 4wt% silica (SiO_2), and 3wt% titanium oxide (TiO_2). A mass loss of 22.5% is observed during calcination studies; this mass loss is attributed to the dehydration and vaporization of volatile impurities. An FTIR study confirms the presence of alumina. The results of this study demonstrate the feasibility of obtaining high alumina extraction yields from low-grade bauxite minerals with high iron contents, which are not readily used for alumina production.

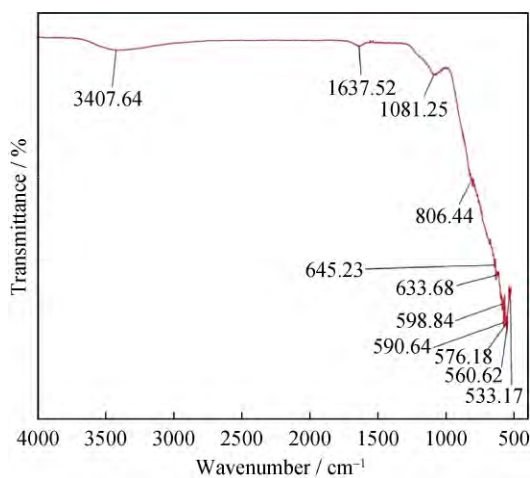


Fig. 12. FTIR of alumina produced by leaching of reduced bauxite.

Acknowledgements

The authors would like to thank the National Aluminium Company (NALCO) for financial support. They also would like to thank Mr. M. Agarwal of SLM Metal (P) Ltd., Rourkela, and Prof. B.K. Mishra, director of Institute of Minerals and Materials Technology (IMMT), Bhubaneswar, for allowing us to conduct the reduction processing of bauxite samples. One author of this manuscript, Mr. B.R. Parhi, would like to thank Dr. R. Bhima Rao, former scientist, and Dr. B.C. Tripathy, scientist, IMMT, Bhubaneswar, for their valuable suggestions while preparing the manuscript.

References

- [1] Technology Information, Forecasting, and Assessment Council (TIFAC) Reports, *Beneficiation of Bauxite for Removal of Iron Oxide*, Technology Information, Forecasting, and Assessment Council, Department of Science and Technology, Government of India, 2001.
- [2] S. Rai, K.L. Wasewar, J. Mukhopadhyay, C.K. Yoo, and H. Uslu, Neutralization and utilization of red mud for its better waste management, *Arch. Environ. Sci.*, 6(2012), p. 13.
- [3] R.K. Paramguru, P.C. Rath, and V.N. Mishra, Trends in red mud utilization: a review, *Miner. Process. Extr. Metall. Rev.*, 26(2004), No. 1, p. 1.
- [4] V.M. Sglavo, S. Maurina, A. Conci, A. Salviati, G. Carturan, and G. Cocco, Bauxite 'red mud' in the ceramic industry: Part 2. Production of clay-based ceramics, *J. Eur. Ceram. Soc.*, 20(2000), No. 3, p. 245.
- [5] D.Q. Zhu, T.J. Chun, J. Pan, and Z. He, Recovery of iron from high-iron red mud by reduction roasting with adding sodium salt, *J. Iron Steel Res. Int.*, 19(2012), No. 8, p. 1.
- [6] G. Power, M. Grafe, and C. Klauber, Application of Bayer red mud for iron recovery and building material production from aluminosilicate residues, bauxite residue issues: I. Current management, disposal and storage practices, *Hydrometallurgy*, 108(2011), No. 1-2, p.33.
- [7] Y.J. Liu and R. Naidu, Hidden values in bauxite residue (red mud): recovery of metals, *Waste Manage.*, 34(2014), No. 12, p. 2662.
- [8] P. Kounalakis, K. Aravossis, and C. Karayianni, Feasibility study for an innovative industrial red mud utilisation method, *Waste Manage. Res.*, 34(2016), No. 2, p. 171.
- [9] A. Pyasi, *Value Added Metal Extraction from Red Mud* [Dissertation], National Institute of Technology, Rourkela, 2014, p. 14.
- [10] C.R. Borra, Y. Pontikes, K. Binnemans, and T.V. Gerven, Leaching of rare earths from bauxite residue (red mud), *Miner. Eng.*, 76(2015), p. 20.
- [11] É.A. Deady, E. Mouchos, K. Goodenough, B.J. Williamson, and F. Wall, A review of the potential for rare-earth element resources from European red muds: examples from Seydişehir, Turkey and Parnassus-Giona, Greece, *Mineral. Mag.*, 80(2016), No. 1, p. 43.
- [12] M.D. Niculescu, Study on chemically modified red mud for pollutants capturing from industrial effluents, *Rev. Chim.*, 65(2014), No. 11, p. 1310.
- [13] M. Shirzad-Siboni, S.J. Jafari, O. Giahi, I. Kim, S.M. Lee, and J.K. Yang, Removal of acid blue 113 and reactive black 5 dye from aqueous solutions by activated red mud, *J. Ind. Eng. Chem.*, 20(2014), No. 4, p. 1432.
- [14] F.M. Kaußen and B. Friedrich, Reductive smelting of red mud for iron recovery, *Chem. Ing. Tech.*, 87(2015), No. 11, p. 1535.
- [15] Z.B. Liu and H.X. Li, Metallurgical process for valuable elements recovery from red mud: a review, *Hydrometallurgy*, 155(2015), p. 29.
- [16] K. Binnemans, P.T. Jones, B. Blanpain, T.V. Gerven, and Y. Pontikes, Towards zero-waste valorisation of rare-earth-containing industrial process residues: a critical review, *J. Clean. Prod.*, 99(2015), p. 17.
- [17] M.J. Ma, G.Y. Wang, Z.P. Yang, S.X. Huang, W.J. Guo, and Y.X. Shen, Preparation, characterization, and photocatalytic

- properties of modified red mud, *Adv. Mater. Sci. Eng.*, 2015(2015), p. 1.
- [18] F.M. Kaußen and B. Friedrich, Methods for alkaline recovery of aluminum from bauxite residue, *J. Sustain. Metall.*, 2016, p. 1.
- [19] K.H. Lim and B.H. Shon, Metal components (Fe, Al, and Ti) recovery from red mud by sulfuric acid leaching assisted with ultrasonic waves, *Int. J. Emerg. Technol. Adv. Eng.*, 5(2015), No. 2, p. 25.
- [20] C.H. Yeh and G.Q. Zhang, Stepwise carbothermic reduction of bauxite ores, *Int. J. Miner. Process.*, 124(2013), p. 1.
- [21] M. Halmann, M. Epstein, and A. Steinfeld, Vacuum carbothermic reduction of bauxite components: a thermodynamic study, *Miner. Process. Extr. Metall. Rev.*, 33(2012), No. 3, p. 190.
- [22] M. Halmann, A. Steinfeld, M. Epstein, E. Guglielmini, and I. Vishnevetsky, Vacuum carbothermic reduction of alumina, *Miner. Process. Extr. Metall. Rev.*, 35(2014), No. 2, p. 126.
- [23] T. Kitamura, K. Shibata, and K. Takeda, In-flight reduction of Fe_2O_3 , Cr_2O_3 , TiO_2 and Al_2O_3 by Ar- H_2 and Ar- CH_4 plasma, *ISIJ Int.*, 33(1993), No. 11, p. 1150.
- [24] B. Bhoi, B.K. Mishra, R.K. Paramguru, S.K. Pradhan, P.S. Mukherjee, S. Sahoo, S. Priyadarshini, P. Rajput, and S.K. Das, *Green Process for the Preparation of Direct Reduced Iron*, US Patent, Appl.US2013/0047782A1, 2013.
- [25] V.A. Lyubochko, V.V. Malikov, O.G. Parfenov, and N.V. Belousova, Reduction of aluminum oxide in a nonequilibrium hydrogen plasma, *J. Eng. Phys. Thermophys.*, 73(2000), No. 3, p. 568.
- [26] D.E. Bullard and D.C. Lynch, Reduction of titanium dioxide in a nonequilibrium hydrogen plasma, *Metall. Mater. Trans. B*, 28(1997), No. 6, p. 1069.
- [27] K.C. Sabat, R.K. Paramguru, S. Pradhan, and B.K. Mishra, Reduction of cobalt oxide (Co_3O_4) by low temperature hydrogen plasma, *Plasma Chem. Plasma Process.*, 35(2015), No. 2, p. 387.
- [28] Y. Nakamura, M. Ito, and H. Ishikawa, Reduction and dephosphorization of molten iron oxide with hydrogen-argon plasma, *Plasma Chem. Plasma Process.*, 1(1981), No. 2, p. 149.
- [29] A. Huczko and P. Meibus, RF plasma processing of silica, *Plasma Chem. Plasma Process.*, 9(1989), No. 3, p. 371.
- [30] W. Zhang, D.R. Sadedin, M.A. Reuter, and J.C. McCallum, The de-oxidation of partially oxidized titanium by hydrogen plasma, *Mater. Forum*, 31(2007), p. 76.
- [31] A.A. Bergh, Atomic hydrogen as a reducing agent, *Bell Syst. Tech. J.*, 44(1965), No. 2, p. 261.
- [32] J.M. Andersson, *Controlling the Formation and Stability of Alumina Phases* [Dissertation], Linköping University, Linköping, 2005, p. 26.
- [33] K. Djebaili, Z. Mekhalif, A. Boumaza, and A. Djelloul, XPS, FTIR, EDX, and XRD analysis of Al_2O_3 scales grown on PM2000 alloy, *J. Spectrosc.*, 2015(2015), p. 1.